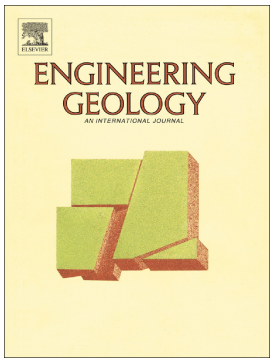

Monitoring the performance of permeable reactive barriers constructed in acid sulfate soils

Subhani Medawela, Buddhima Indraratna, Senura Athuraliya, Glenys Lugg, Long D. Nghiem

PII: S0013-7952(21)00476-2

DOI: https://doi.org/10.1016/j.enggeo.2021.106465

Reference: ENGEO 106465

To appear in: *Engineering Geology*

Received date: 14 December 2020

Revised date: 12 November 2021

Accepted date: 14 November 2021

Please cite this article as: S. Medawela, B. Indraratna, S. Athuraliya, et al., Monitoring the performance of permeable reactive barriers constructed in acid sulfate soils, *Engineering Geology* (2021), https://doi.org/10.1016/j.enggeo.2021.106465

Monitoring the Performance of Permeable Reactive Barriers constructed in Acid Sulfate Soils

Subhani Medawela, PhD[a], **Buddhima Indraratna[b]**, **Senura Athuraliya[c]**, **Glenys Lugg[d]**, **Long D. Nghiem[e]**

[a]Postdoctoral Research Fellow, Faculty of Engineering and Information Technology, University of Technology Sydney, NSW 2007, Australia
Email: subhani.medawela@uts.edu.au

[b]PhD, FTSE, FIEAust, FASCE, FGS, CEng., CPEng, Distinguished Professor of Civil Engineering, Director of Transport Research Centre (TRC), Faculty of Engineering and Information Technology, University of Technology Sydney, NSW 2007, Australia
Email: buddhima.indraratna@uts.edu.au

[c]PhD Candidate, Faculty of Engineering and Information Technology, University of Technology Sydney, NSW 2007, Australia
Email: senura.h.athuraliya@student.uts.edu.au

[d]Environmental Scientist, Manildra Group Shoalhaven Starches Pty Ltd, 36 Bolong Road Bomaderry NSW 2541
Email: glenys.lugg@manildra.com.au

[e]B.Eng (UNSW), Grad. Cert., M.Edu, PhD (UOW), Professor in Environmental Engineering, Head of Discipline, Environmental & Water Engineering, Director, Centre for Technology in Water and Wastewater Treatment (CTWW), Faculty of Engineering and Information Technology, University of Technology Sydney, NSW 2007, Australia
Email: DucLong.Nghiem@uts.edu.au

Abstract

Two pilot-scale permeable reactive barriers (PRBs) were installed in an acidic terrain to treat contaminated groundwater with low pH and high concentrations of Al and Fe. The first pilot-scale barrier (PRB-1) was installed in 2006 using recycled concrete aggregates (RCA) as the reactive material, and the second barrier (PRB-2) was installed in late 2019 using limestone aggregates (LA) as the reactive material. Although the initial material cost of the recycled concrete aggregates is low, laboratory trials conducted before the field applications deduced that limestone is capable of more reliable and efficient pH neutralisation in the long term, reducing frequent maintenance or material replacement in the PRB. The performance of PRB-1 has been monitored continuously over the past 14 years. In particular, both internal (within PRB) and external (upgradient and downgradient) variations in acidity (pH), ion concentrations, and the flow conditions, including the piezometric heads, have been analysed. These decade long field observations have resulted in a comprehensive understanding of the temporal variations of treatment by RCA along the groundwater flow path through the alkaline granular mass and its biogeochemical clogging. For instance, acid neutralisation at

the entrance of PRB-1 decreased by 31% over 14 years, whereas the corresponding reduction at the outlet is only 6%. The non-homogeneous biogeochemical clogging in different PRB zones was evident by a 48% reduction in hydraulic conductivity at the inlet and a 34% reduction at the outlet.

Keywords

Permeable reactive barriers, Acid sulfate soils, Groundwater, Biogeochemical clogging, Acidity

1. Introduction

Acid sulfate soils occupy approximately 215,000 km^2 of land in Australia (Fitzpatrick et al. 2011). Shallow pyrite deposits (FeS_2) in these acidic floodplains oxidise when they are exposed to the atmosphere during prolonged dry weather conditions and due to ground disturbances caused by construction of infrastructure and mining activities (Shand et al. 2018). The oxidation of acid sulfate soils produces sulfuric acid, which significantly reduces the pH of surrounding soil and groundwater (pH~3) and causes metals such as aluminium (Al) and iron (Fe) to leach out. Acidic water with high levels of Al and Fe is corrosive and poses a severe threat to the environment and infrastructure (Groeger et al. 2008; Högfors-Rönnholm et al. 2018; Medawela et al. 2019).

Permeable reactive barriers (PRBs) are a passive method for treating contaminated groundwater. A PRB is an underground granular filter with reactive material that can contain or eradicate the contaminants in groundwater through chemical and/or biological processes (Gillham et al. 2010; Hoppe et al. 2011). Following installation, a PRB must be monitored continuously over the years because its efficiency is affected by changing weather conditions and unpredicted fluctuations in the chemical composition of influent water. These natural variations are difficult to capture in laboratory experiments carried out under controlled conditions (constant flowrate and hydrochemistry) or numerical modelling during the PRB design stage (Gibert et al. 2019; Medawela & Indraratna 2020). Moreover, the chemical and biological clogging of a PRB can drastically reduce its porosity and hydraulic conductivity, and thus its longevity (Ekolu & Bitandi 2018; Maamoun et al. 2020); hence it is crucial to quantify PRB clogging based on real-time data. For instance, chemical precipitates form in a PRB installed in an acidic terrain when the alkaline material in the PRB reacts with the acidic water. These precipitates can encrust the reactive surfaces of the aggregates (known as chemical armouring) (Cravotta & Watzlaf, 2002) and also accumulate within the porous matrix of the barrier (known as chemical clogging) (Li et al. 2006; Indraratna et al. 2019). In addition, bacterial strains that reside in pyritic soils can also enter the PRB with the groundwater and grow within the voids, thus clogging the PRB biologically (Indraratna et al. 2020).

Due to time limitations, most studies reported in the literature only examined the performance of PRBs during the first 5-6 years of operation (Puls et al. 1999; Blowes et al. 2000; Bain et al. 2006; Jeen et al. 2011; Gibert et al.2019). A PRB generally takes about a year to stabilise

after being installed, so clogging is not significant during the first few years. However, noticeable changes in hydraulic conductivity and porosity can occur later as clogging progresses towards the outlet; this means the PRB would fail to remove contaminants from groundwater up to required standards. Therefore, for the first time in Australia, this paper evaluates a significant amount of field data collected over 14 years from a pilot scale PRB installed in a coastal acidic floodplain in an attempt to examine the mechanism of acid neutralisation and metal removal by the selected reactive material under natural flow conditions. Moreover, data were analysed to understand the bio-geochemical clogging patterns of the granular assembly to determine whether the pilot scale PRB reached the threshold limit at which the depleted granules should be replaced to maintain the efficiency of the PRB.

2. Study Site

The study site is located in farming land situated in the lower Shoalhaven floodplains, 130 km south of Sydney, Australia. The site is adjacent to a flood mitigation drain that flows into Broughton creek, a tributary of the Shoalhaven River.

The ideal pH recommended for water bodies in Australia is between 6.5 and 8.5; this pH is suitable for flora and fauna and also minimises corrosion and scaling of pipes and fittings (NRMMC 2011). Australian and New Zealand guidelines for fresh and marine water quality (ANZECC 2000) recommend that the maximum acceptable concentrations of Al and Fe in surface water bodies should be less than 0.54 mg/L and 0.5 mg/L, respectively. The pH and concentrations of cations and anions of groundwater at this site were examined for the past 15 years (Golab et al. 2006a; Indraratna et al. 2010; Indraratna et al. 2014a; Indraratna et al., 2020). The results confirmed that the average pH (~3.8) and dissolved concentrations of Al (54 mg/ L) and Fe (91 mg/ L) in the groundwater (Table 1) do not meet the regulatory standards, so two pilot-scale PRBs were installed approximately 15 m away from the flood mitigation drain. The main objectives of these pilot-scale PRBs were to finalise an effective reactive material that would remove acidity and excessive concentrations of Al and Fe from the contaminated groundwater as well as understand the clogging mechanisms. These are critical factors when designing large-scale PRBs to treat acidic groundwater. The location for the

pilot-scale PRBs was selected after evaluating the hydrogeological parameters of this site, such as the phreatic surface variations and hydraulic conductivity of soils, and based on finite

element modelling (Seep 2D), to direct the maximum flow of contaminant plume towards the PRB (Golab et al. 2006a). The treated effluent flowing out of these pilot-scale PRBs may mix with pyritic soils in the far downgradient and generate some acidity due to their scaled-down width. However, this effect could be eliminated in a full-scale PRB, where the scale of treatment width and barrier length would be much greater to cater for a much larger ground area.

2.1 Construction of PRBs

The first pilot-scale PRB was installed in October 2006 using recycled concrete aggregates (RCA) as the reactive material; it is referred to as PRB-1 in this paper. Its construction procedure was presented by Indraratna et al. (2014a). The 10 m long PRB-1 was extended northbound in 2019 [Figure 1 (a)], using limestone aggregates (LA) as the reactive material; it is referred to as PRB-2 in this paper. The construction procedure of PRB-2 and the reason to trial LA in PRB-2 are described in the subsequent sections of this paper. PRB-1 and PRB-2 have similar dimensions (18 m x 1.2 m x 3 m). The treatment and direction of groundwater flow within both PRBs are along their width, which is 1.2 m (Figure 2). This optimum barrier thickness is assessed based on criteria explained by Pathirage & Indraratna (2014). The average depth of the groundwater table in PRB upgradient is 0.75 m; thus, the depth of the barriers was selected as 3 m to ensure that acidic water does not pass under the PRB. The minimum water table depth at upgradient recorded during the past 14 years was 0.21 m from the ground surface, and the maximum was 1.8 m.

PRB-2 was constructed using the cut and fill method. Excavation commenced where PRB-1 ended [Figure 1(a)], without disturbing its reactive aggregates or the geo-fabric wrapping. The soil at this study site has a low undrained shear strength (< 10 kPa), so steel shoring was placed along the edges of the trench to prevent the walls from collapsing [Figure 1(b)]. Because the ground is soft and clayey, a 300 mm thick rock fill was placed at the bottom of the channel as a firm base. An impervious 1 mm thick HDPE membrane was laid on the floor. Then a nonwoven geotextile (150 gsm) was placed on top of the HDPE membrane and over the walls of the trench to prevent debris and soil from entering the PRB and being carried along with groundwater and result in physical clogging [Figure 1(c)]. The trench was then backfilled with limestone up to 500 mm thickness [Figure 1(d)].

Observation wells (OWs), standpipe piezometers, and data logger wells were aligned and placed on top of the 500 mm limestone backfill [Figure 1(d)] to ensure they all reached a depth of 2.5 m from ground level. Instruments were installed along five transects (T1-T5 in Figure 3) that are approximately parallel to the groundwater flow to enable observations from the inlet, middle, and outlet of the PRB. The remaining depth was then filled with limestone to approximately 200 mm below the ground surface. The shoring was then removed, and the geotextile was wrapped over the top of the barrier to protect the limestone aggregates from excessive movement away from the boundary of the trench [Figure 1(e)]. The soil taken out from the trench was placed on top of the barrier, levelled with the existing ground surface, and then lightly compacted. After levelling the ground, hydrated lime was spread over the site to prevent any problems from excavating pyrite deposits from the in-depth profile. After constructing the barrier, instruments were installed along the extended transects on the upgrade and downgrade from the PRB [Figure 2].

The field instruments on the five transects enable water quality (pH, oxidation-reduction potential (ORP), the electrical conductivity (EC), and the dissolved oxygen (DO)) along a specific horizontal flow path to be analysed from upgradient to downgradient. This is vital for understanding the treatment patterns in different zones of the pilot-scale PRB (e.g. inlet, middle and outlet) and validating the numerical models that simulate the behaviour of a PRB. The monitoring network of both PRBs is shown in Figure 3. Details of the instrumentation and monitoring framework used for both PRBs are listed in Table 2.

3. Selecting reactive materials

Before installing the PRBs at the selected site, laboratory tests were carried out to select a suitable reactive material and understand the chemical and biological reactions between the reactive material and target contaminants. Golab et al. (2006b) conducted batch tests to screen 25 alkaline materials for treating acidic groundwater in the study site. They found that lime, recycled concrete, fly ash, blast furnace slag and limestone could neutralise acidity, but some materials were eliminated due to very small grain sizes (e.g. lime and fly ash), insufficient acid neutralising capacity, and insufficient removal of Al and Fe. Following the initial screening, Indraratna et al. (2014b) and Indraratna et al. (2020) conducted long-term laboratory column experiments to investigate the potential of RCA and LA to remove acidity, Al, and Fe from the groundwater at the selected site. Acrylic columns (diameter 50 mm, length 500 mm) were filled with 5 mm aggregates, and then synthetic acidic groundwater that

mimics the groundwater chemistry at this site (Table 1) was pumped through these horizontal columns at a flow rate of 1.2 mL/min. The pH of the column effluents was plotted against time (Figure 4).

3.1 Recycled concrete aggregates (RCA)

The recycled concrete aggregates (RCA) used in PRB-1 and column experiments was sourced from a refuse depot containing concrete elements used previously in road expansion works in rural NSW. Because this waste concrete mixture is heterogeneous, the accurate characterisation of this material and the age of different elements in the mixture are unknown. However, past local government council reports suggested that most of these elements belonged to concrete grades M25 and M30 with a water/cement ratio of 0.4 – 0.43 (Banasiak et al. 2013).

Regmi et al. (2009) conducted inductively coupled plasma-mass spectrometry (ICP-MS) to analyse the chemical composition of the selected RCA mixture. It was found that the RCA contained 57.3% of Ca, 21.4% of Fe, 9.83% of Al, 5.27% of Mg, 3.06% of Si and 3.04% of other metals by weight. X-ray fluorescence (XRF) of the RCA mixture proved the presence of SiO_2 (66.2 %), CaO (9. 79%), Al_2O_3 (7.51%) and Fe_2O_3 (3.54%) (Regmi et al. 2011; Banasiak et al. 2013). The most common alkalinity generating agents in concrete are cementitious minerals because large amounts of calcium oxide are found in cement in complex forms such as calcium silicate hydrated compounds (CSH), calcium hydroxide ($Ca(OH)_2$) and calcium aluminosilicate hydrated compounds (CAH). Quantitative x-ray diffraction (XRD) results (Regmi et al. 2011) confirmed the presence of these cementitious minerals [portlandite ($Ca(OH)_2$), anorthite ($CaAl_2Si_2O_8$), and calcite ($CaCO_3$)] in this batch of RCA (Table 3). There is a significant composition of quartz due to the presence of sand and aggregate in concrete, but SiO_2 is chemically inert in acid neutralisation reactions.

The dissolution of the cementitious minerals in the presence of CO_2 and moisture can release large amounts of Ca and generate alkalinity to neutralise the pH of pore water. Some calcium carbonate may have already formed in the RCA due to the carbonation of hydrated cement products, as shown in Eq.1 and 2 (Goyal & Sharma, 2020):

$$Ca(OH)_{2(s)} + CO_2 \rightarrow CaCO_3 + 2H_2O$$
(1)

$$CSH + CO_2 \rightarrow CaCO_3 + H_2O + SiO_2$$
(2)

According to Eq.3 (Sephton & Webb, 2019), the dissolution of minor amounts of portlandite in the acidic groundwater could be the reason for the rapid increase of pH up to 9.2 at the beginning of the test (Figure 4).

$$Ca(OH)_2 + 2H^+ \leftrightarrow Ca^{2+} + 2H_2O$$
(3)

The amount of portlandite was low (0.3% by weight) in this particular batch of RCA, so the dissolution of portlandite could not buffer the pH for very long, which could be attributed to the rapid drop of pH from 9.2 to 8.0 in 10 days. Moreover, the total alkalinity could also decrease due to the precipitation of calcite during this state of buffering. Once the portlandite ($Ca(OH)_{2(s)}$) in concrete is exhausted, the CSH compounds are expected to play a crucial role in buffering the pH (Baston et al. 2012). The dissolution of CSH can be described as (Berner, 1988, Harris et al. 2002):

$$[xCaO.SiO_2.yH_2O]_{(s)} \rightarrow [(x-a)CaO.(1-b)SiO_2.(y-a)H_2O]_{(s)} + aCa(OH)_2 + bSiO_2$$
(4)

While the dissolution of CSH compounds (Eq. 4) produces $Ca(OH)_2$, which can release Ca (Eq.3), the progressive dissolution of anorthite ($CaAl_2SiO_8$) and calcite ($CaCO_3$) also supported an almost neutral pH range (6.8 < pH < 7.9) from Day 12 to Day 63 (Figure 4), as the continuous dissolution of these Ca-rich minerals released calcium and generated bicarbonate alkalinity (Eq. 5-7). Afterwards, the pH of the effluent dropped abruptly to 4.2, probably due to the depletion of alkalinity in the RCA column.

$$CaAl_2Si_2O_8 + 8H^+ \rightarrow Ca^{2+} + 2Al^{3+} + 2H_4SiO_4$$
(5)

$$CaCO_3 + 2H^+ \leftrightarrow Ca^{2+} + H_2CO_3$$
(6)

$CaCO_3 + H_2CO3 \leftrightarrow Ca^{2+} + 2HCO_3^-$ (7)

3.2 Limestone aggregates (LA)

The limestone aggregates used in PRB-2 and column experiments were procured from a quarry at Moss Vale, Australia. Crystallised $CaCO_3$, rather than overburden limestone, was selected. The limestone consisted of 98.2% $CaCO_3$ (Table 4), which was confirmed using XRD analysis. This large amount of calcite dissolves when exposed to acidic groundwater and produces dissolved Ca and CO_2 (Eq.6). Dissolved CO_2 is a weak acid that continues to react with limestone to produce calcium and bicarbonate alkalinity (Eq.7), which is available for acid neutralisation (Cravotta & Trahan, 1999). Basically, the lower the pH, the higher the concentration of bicarbonate; this shows how a lower pH can lead to higher alkalinity if the amount of bicarbonate produced is greater than the amount of H^+ remaining after the reaction. For instance, the initial pH of the limestone column effluent was high (pH= 8) and gradually reduced to 6.8 in 20 days as the column became stable; it then maintained a near-neutral pH plateau (6.5 < pH < 6.8) from Day 20 to Day 97 (Figure 4) due to prolonged bicarbonate buffering.

The RCA maintained higher initial alkalinity than the LA, but this led to the initial pH of RCA column effluent (pH = 9.2) increasing beyond acceptable limits (> 8.5), while the acceptable pH range (6.5 < pH < 8.5) only lasted until Day 63 (Figure 4). In contrast, the LA maintained the pH of the effluent within the standard range from the beginning of the test until Day 97. The RCA column effluent swiftly reached the influent pH (pH = 3.8) after 90 days, while the LA column effluent slowly reached the influent pH after 256 days with fewer fluctuations in the pH profile, which infers that limestone could generate prolonged alkalinity compared to waste concrete aggregates. In addition to these experimental observations, Medawela & Indraratna (2020) used finite-difference modelling to simulate the behaviour of two pilot-scale PRBs and confirmed the consistent and prolonged treatment by LA compared to the short-term near-neutral effluent pH maintained by RCA.

Furthermore, the consistent and long-lasting treatment by limestone is advantageous in PRB maintenance because the frequency of replacing old aggregates, which no longer provide a neutralised effluent, could be reduced or might not be necessary for many years. Even though the RCA is eco-friendly, and the initial material cost could be lower because they were

sourced from a waste plant, if the effluent pH began to drop below the standard margin after only a few years of operation, frequent maintenance of the PRB and material replacement, or installing a new PRB might be required, which would be much more expensive. Material replacement is generally required only at the PRB inlet because this entrance zone gets armoured and clogged faster than the adjacent middle and outlet zones, as explained in subsequent sections of this paper. Therefore if the material must be replaced at the inlet after a few years, finding RCA with similar mineralogy to the first batch (i.e. similar to RCA in middle and outlet aggregates) would be difficult. This is because RCA does not have consistent properties compared to locally quarried limestone aggregates. Depending on the demolition sites (age and type of concrete mix constituents), the properties of RCA change considerably. In order to check whether the new batch of RCA is capable of acid neutralisation while removing Al and Fe, the column tests must be repeated. Moreover, what is used in small quantities for experimental work may be completely different to RCA obtained in very large quantities for the field PRB (may have to be sourced from different sites). Therefore, as a novel material that could maintain the effluent pH within the applicable limits in the long term, limestone was trialled in PRB-2.

4. Monitoring the performance of PRB-1

4.1 Upgradient water quality

The average pH of the upgradient was determined after measuring the pH in all OWs installed in the upgradient of PRB-1 [Figure 5(a)]. The upgradient pH fluctuates continuously with time and is always acidic. During dry periods with no or low rainfall, the water table would recede further down [Figure 5(b)], thus exposing the shallow pyrite layers in the floodplain to the atmosphere, such that FeS_2 would oxidise (Nordstrom 1982; Rimstidt & Vaughan 2003):

$$FeS_{2(s)} + \frac{7}{2}O_{2(aq)} + H_2O \rightarrow Fe^{2+} + 2SO_4{}^{2-} + 2H^+ \quad (8)$$

Ferrous ions, in the presence of oxygen, oxidise to ferric (Eq. 9), and Fe^{3+} hydrolyses to form insoluble ferric hydroxide at pH greater than 3.5, thus generating more acidity (Eq. 10).

$$Fe^{2+} + \frac{1}{4}O_{2(aq)} + H^{+} \rightarrow Fe^{3+} + \frac{1}{2}H_2O$$
(9)

$$Fe^{3+} + 3H_2O \rightarrow Fe(OH)_3 + 3H^{+}$$
(10)

After the initiation of pyrite oxidation at low pH, the ferric ion could be reduced by pyrite itself faster than by O_2 (Eq.11), thus generating more acidity in the soils (Singer & Stumm, 1970):

$$FeS_{2(s)} + 14Fe^{3+} + 8H_2O \rightarrow 15\,Fe^{2+}{}_{(aq)} + 2SO_4{}^{2-} + 16H^{+}$$
(11)

The data obtained so far indicate that the average concentration of Al (32 mg/L) in the upgradient water was higher by several orders of magnitude than the acceptable limit of 0.54 mg/L (Figure 6). The toxicity of Al at the Shoalhaven floodplain increases when the silicate clays and Al-bearing minerals dissolve under acidic groundwater conditions (Blunden & Indraratna, 2000). Moreover, over the past 14 years, the concentration of total Fe in the upgradient ranged from a minimum of 4.5 mg/L to a maximum of 295 mg/L with an average of 103 mg/L (Figure 6).

4.2 Groundwater treatment by PRB-1

Seven months after installing PRB-1, the effluent pH reached a peak of 10.2 and then stabilised in a near-neutral pH range (6.6 < pH < 7.7) after almost one year of operation [Figure 5 (a)]. These variations of pH are caused by the dissolution of cementitious minerals in the RCA (Eq. 1-7), as explained in Section 3.1. However, other than the chemical reactions between RCA and acidic groundwater, the pH in the PRB could fluctuate during the initial stage before stabilising due to dewatering during construction and subsequent changes in hydraulic gradient (hydraulic conductivity of the soil at the site = 10^{-5} m/s, hydraulic conductivity of the RCA used in PRB-1=1.1 x10^{-1} m/s); this could cause the PRB to act as a sink due to its ability to absorb water. Changes in rainfall also play a major role in saturating the PRB and subsequent stabilisation; for instance, heavy rainfall in February 2007 could have saturated PRB-1 and allowed the effluent pH to gradually stabilise within the acceptable range.

Aluminium begins to precipitate when the pH rises above 4.5 according to Eq.12 (Cardiano et al. 2017), whereas Fe precipitates when the pH exceeds 3.5 according to Eqs 13-17 (Balintova & Petrilakova, 2011). Given that the pH within PRB-1 was always observed to be above 4.5 up to the current date [Figure 5(a)], the Fe and Al in the groundwater were expected to leave the solution by making precipitates in the form of oxides and hydroxides. This means the significant reductions in Al and Fe concentrations in specimens taken from PRB-1 compared to the unacceptably higher concentrations in the upgradient (Figure 6) could be attributed to the formation of secondary mineral precipitates (Eq. 12-17).

$$Al^{3+} + 3H_2O \rightarrow Al(OH)_{3(s)} + 3H^+_{(aq)} \quad (12)$$

$$Fe^{3+} + 3H_2O \rightarrow Fe(OH)_{3(s)} + 3H^+_{(aq)} \quad (13)$$

$$Fe^{3+} + 2H_2O \rightarrow FeO(OH) + 3H^+_{(aq)} \quad (14)$$

$$2Fe^{3+} + 3H_2O \rightarrow Fe_2O_3 + 6H^+_{(aq)} \quad (15)$$

$$Fe^{2+} + 2(OH)^- \leftrightarrow Fe(OH)_2 \quad (16)$$

$$Fe^{2+} + CO_3^{2-} \leftrightarrow Fe(CO)_{3(s)} \quad (17)$$

Unlike the significant reductions in concentrations of Al and Fe in PRB-1, there were no significant changes in the concentration of Na^+, K^+, Mg^{2+}, Cl^- and SO_4^{2-} in groundwater within the PRB-1, compared to their concentrations upstream (Figure 7). This indicates that these ions were not affected by the neutralising reactions that occurred in PRB-1.

4.3 Numerical Analysis of Geochemical Speciation

The saturation indices (SI) can be used to explain the precipitation and dissolution of minerals in PRB-1 (Eq.18), which had been previously inferred based on the reduction of dissolved concentrations of Al and Fe in the groundwater samples (Figure 6).

$$SI = \log(IAP) - \log(K_{eq}) \quad (18)$$

where SI is the saturation index, IAP is the ion activity product, and K_{eq} is the solubility constant.

When a system is not in equilibrium, the degree of disequilibrium can be expressed through the saturation index, so when SI > 0 (supersaturation), the mineral tends to precipitate, but when SI = 0, the mineral and the solution are in equilibrium, and when SI < 0 (undersaturation) the mineral tends to dissolve. The saturation index of various mineral phases of PRB-1 effluent was calculated by the geochemical speciation/mass transfer computer code PHREEQC (Version. 3.3.12). It is based on a geochemical mole balance model, which indicates the moles of minerals and gases that may enter or leave a solution due to differences between the initial and final chemical composition of the solution flowing on a surface or underground system (Parkhurst & Appelo, 1999). The input parameters of PHREEQC to calculate the SIs were the concentrations of Al^{3+}, Fe, Ca^{2+}, Na^{+}, K^{+}, Mg^{2+}, Cl^{-}, SO_4^{2-}, pH, ORP, and temperature of the groundwater.

The precipitation of Al minerals [alunite ($KAl_3(SO_4)_2(OH)_6$)], gibbsite ($Al(OH)_3$), $Al(OH)_{3(a)}$] and Fe minerals [goethite ($FeOOH$), hematite (Fe_2O_3), and $Fe(OH)_3$] was affirmed by the positive saturation indices [Figure 8(a) and (b)]. The dissolution of Ca-rich minerals in RCA was evident from the negative saturation indices [Figure 8(c)]. According to Figure 7(e), the concentration of SO_4^{2-} in upgradient groundwater did not change significantly after passing through PRB-1, suggesting that gypsum had not precipitated. Gypsum remained unsaturated in PRB-1 [(Figure 8(c)], probably due to insufficient amounts of SO_4^{2-} in the influent to reach the solubility product of gypsum in equilibrium. This supposition is supported by a study involving another passive treatment system where the concentration of SO_4^{2-} required for gypsum to precipitate was greater than 2000 mg /L (Robbins et al. 1999). In the current study, the maximum concentration of SO_4^{2-} recorded in the upgradient during the last 14 years was 1235 mg/L [Figure 7(e)]. Bellmann et al. (2006) also studied gypsum precipitation in concrete elements in contact with solutions of different concentrations of SO_4^{2-} and suggested that until these concentrations increased beyond 3000 mg/L, the formation of gypsum under most of the field conditions is not possible.

4.4 The Growth of Bacteria in PRB-1

The most common strain of iron oxidising bacteria (IOB) found in the Shoalhaven floodplain is *Acidithiobacillus ferrooxidans* (Indraratna et al. 2020). These bacteria enter the PRB with groundwater and continue to multiply as they thrive on the energy derived from redox reactions they catalyse (Eq.9). When bacteria grow on RCA surfaces and the voids of the granular matrix, PRB is clogged biologically, and when they catalyse the oxidation of Fe^{2+} into Fe^{3+} (Eq. 9), the formation of Fe precipitates is accelerated (Nordstrom, 1982; Rawlings, 2002). Figure 9 shows the concentration of *Acidithiobacillus ferrooxidans* in water samples obtained from PRB-1. Data on the population of bacteria are only available from January 2017 because previous research work did not evaluate the biotic role inside PRB-1; it only focused on chemical clogging. However, biological clogging in a PRB is an influential factor in determining its efficiency (Indraratna et al. 2020). The bacterial cell count for this particular strain of IOB was always higher at the PRB inlet because the optimum growth conditions were met. For example, a low pH (<2.5) is required for the growth of *Acidithiobacillus ferrooxidans* and Fe^{2+} acts as an electron acceptor for its metabolism (Pronk et al. 1992; Rawlings 2002). Therefore, the increase of pH and reductions in the concentrations of Fe towards the outlet (Figures 10 and 11) may be the reason for this trend of bacterial growth.

4.5 Change of treatment along the PRB

The pH and dissolved Ca, Al, and Fe concentrations of the groundwater specimens taken from the inlet (0 m - 0.4 m), middle (0.4 m – 0.8 m), and outlet (0.8 m – 1.2 m) of PRB-1 differed from zone to zone (Figures 10 and 11), suggesting that the acid neutralisation and metal removal by RCA along the groundwater flow path are not uniform. For instance, the initial peak in pH, which could be attributed to the dissolution of portlandite in RCA (Eq. 3), was observed in the inlet zone five months after installation (pH = 9.4). However, this peak in the middle (pH = 9.7) and outlet zones (pH = 10.2) was seen after six and seven months, respectively. These differences in the zonal pH could have been occurred due to varying alkalinity levels in each zone. For instance, the average concentration of Ca in the upgradient was 128 mg/L during the first year of PRB operation, but after entering the PRB, this value increased up to 378 mg/L at the inlet [Figure 11(a)] because the RCA dissolves rapidly in acidic water (pH = 3.8) and releases Ca bearing minerals (Eq. 1-7). Due to the increased alkalinity at this entrance zone, the pH of the water flowing through it increases. Hence, RCA in the middle zone exposes to less acidic water compared to the inlet aggregates. As

explained in Section 3.2, this increased pH at the middle zone could have resulted in a lesser concentration of dissolved Ca (361 mg/L) compared to the inlet ([Ca] =378 mg/L) at the end of the first year. However, the dissolution of RCA and reducing the acidity of water continues at the middle zone before it flows into the outlet zone, exposing the RCA at the PRB outlet to a minimum acidity. The higher pH at the outlet could have caused the lesser concentration of dissolved Ca (352 mg/L) than the inlet and middle zones at the end of the first year of PRB operation [Figure 11(a)], while the clogging and armouring of the PRB were still not severe. Nevertheless, when armouring and clogging increase with time due to the continuous passage of acid, the coating of the aggregate surfaces hinders the dissolution of RCA mainly at the inlet, causing reduced dissolved Ca concentrations. Therefore although the concentration of Ca at the inlet was higher than the middle and outlet regions in the early stages, it fell below the concentrations in the middle and outlet regions after four years of PRB operation [Figure 11(a)].

Furthermore, in the first year after the PRB had stabilised (i.e. from May 2007 to May 2008) compared to the average upgradient pH (pH =3.8), the percentage increase in groundwater pH at the inlet was 93% (from pH = 3.8 to pH = 7.4), while at the outlet, this increase of pH was 91% (from pH = 3.8 to pH = 7.2). However, in the 14th year (i.e. in 2020), compared to the average upgradient pH ((pH =3.8), the percentage increase of pH at the inlet was only 62% (from pH = 3.8 to pH = 6.2), while at the outlet the increase was 85% (from pH = 3.8 to pH = 7.01) (Figure 10). Thus the acid neutralisation at the inlet decreased by 31% in 14 years, whereas the reduction at the outlet was only 6%. These results suggest that the continuous acidic influent and clogging decrease the effectiveness of RCA towards the inlet, which is further evident by reduced concentrations of Ca and increased concentrations of Al and Fe at the inlet after 14 years of operation (Figure 11). Therefore, similar to the varying acid neutralisation and metal removal from zone to zone, the clogging and armouring towards the outlet was also not uniform. Thus, although the treatment capacity of the inlet diminishes with time due to armouring and clogging, the outlet is still capable of producing an effluent that meets environmental standards over a long period.

The armoured aggregates extracted from the inlet of PRB-1 in December 2019 were observed under scanning electron microscopy (SEM) with energy-dispersive x-ray spectroscopy (EDS) analysis (JSM-6490LA- JOEL). The differences in the surfaces of the RCA before being used in PRB-1 [Figures 12 (b) and (c)] and after armouring [Figure 12 (e) and (f)] were evident in the results. The surface of the RCA before being used in PRB-1 was clear, but the surface of

armoured aggregates could not be seen clearly in the SEM images because the samples were coated. The peaks of the EDS diffractograms confirmed the presence of Al and Fe minerals in the coated aggregates [Figure 12 (d)], but they were absent in the RCA before being used in PRB-1 [Figure 12 (a)].

Since May 2017, i.e. after more than 11 years of operation, the average pH in all three zones of PRB-1 has slightly decreased (Figure 10), and the concentrations of dissolved Al and total Fe [Figures 11 (b) and (c)] have increased. Armouring and clogging and the elevated acidity of the influent during dry weather could be the reasons for these changes. The rainfall data in the study area (see Figure 5) indicate that the minimum rainfall within the previous 14 years was from May 2017 until December 2019; this could have decreased the upgradient pH (Eq. 8-11) and increased the acidity within PRB-1. For instance, the lowest annual rainfall over the past 14 years (509 mm) was recorded in 2019 [Figure 5(b)], where the average depth of the water table was 1.28 m, the lowest annual average depth recorded. In the same year, the PRB-1 influent was the most contaminated, recording the lowest pH in the upgradient (average pH =3.4) and the highest concentrations of Al (average of 42.5 mg/L) and Fe (average of 182.2 mg/L). The elevated acidity of the influent in dry weather from May 2017 until December 2019 seems to have encouraged the bacterial growth (Figure 9), which then catalysed the oxidation of Fe^{2+} to form more iron precipitates.

A decreasing pH and increasing concentrations of ions at the entrance zone infer a depletion in alkalinity and considerable armouring, which means the inlet granules may need to be rejuvenated. However, the effluent of PRB-1 was still producing a neutral effluent that agreed with the standards. Therefore the depleted reactivity at the inlet did not appear to have harmed the overall performance of the PRB over the past 14 years. Although the aggregates at the inlet do not need to be replenished at present, the behaviour of the PRB must be examined to determine when the effluent pH would begin to drop significantly and continuously below the neutral pH and when the concentration of effluent ions would surpass the standards. Before the effluent water quality of PRB-1 becomes poor, replacing the coated aggregates at the inlet with fresh material would renew the alkalinity levels and maintain the quality of the effluent.

4.6 Hydraulic conductivity of PRB-1

The hydraulic conductivity in PRB-1 (Figure 13) was calculated using data collected by standpipe piezometers installed along each of the transect lines (see Figure 3) that are parallel to the groundwater flow through PRB-1. The piezometer data indicated the pressure head in the inlet and outlet of PRB-1. The datum for calculating the hydraulic head in these two zones was assumed to be at a depth of 2.5 m from the ground surface. The hydraulic conductivity was then calculated using Darcy's law. After 14 years of operation, the hydraulic conductivity of the inlet had decreased by 48 % and by 34% in the outlet. These results further prove there was a large degree of biogeochemical clogging at the inlet and a progressive decline towards the outlet. The rate at which the hydraulic conductivity at the inlet area decreased had increased slightly from mid-2017, possibly due to the drop in pH and increased clogging and armouring at the inlet after mid-2017, as explained in Section 4.5.

4.7 Downgradient water quality of PRB-1

The average pH of downgradient water within 7 m from the PRB outlet was at or above 6.5 (see Figure 5); however, the downgradient pH started to drop after May 2017. Mixing the treated effluent with in-situ acid generated due to oxidation of pyrite deposits in downgradient soils, especially during the dry season recorded from 2017 to 2019 (Section 4.5), could be the main reason for this natural reduction of the downgradient pH. However, the main objective of this pilot-scale PRB was to understand the mechanisms of acidic groundwater neutralisation, metal removal and clogging of RCA granular mass. Due to the scaled-down width of the pilot PRB, it is inevitable that the pH of the water flowing away from the pilot-scale PRB has been eventually reduced by rebuilt acidity and mixing with untreated crossflows. When constructing large scale PRBs for industrial use, the downgradient water quality could be enhanced by increasing the barrier width based on accurate calculations and numerical modelling (hybrid model for flow and contaminant transport), as suggested by Pathirage & Indraratna 2015 and Medawela & Indraratna 2020. Also, if PRBs are constructed in series or using a funnel-and-gate design, it could further decrease the risk of mixing the effluent with untreated groundwater.

5. Monitoring the Performance of PRB-2

While PRB-1 was stabilising, the pH and concentrations of effluent ions fluctuated; they did not follow a fixed trend until the end of the first year of construction (see Figure 5). Similar conditions occurred in PRB-2, installed in December 2019, until it became saturated after a

heavy rainfall event in February 2020 (Figure 14). The peak pH recorded while reaching equilibrium was 8.45, which is within the standard pH margin. Currently, the pH in the PRB-2 is plateauing between 6.6 < pH < 7 due to the bicarbonate buffering of LA (Eq. 6 and 7). Based on the laboratory observations (see Section 3), it is expected that this pH plateau of PRB-2 would last longer than the effluent pH profile of PRB-1. Data collected from PRB-1 over the past 14 years were critical in examining the accuracy of the flow and contaminant transport models developed by Medawela & Indraratna (2020) for predicting the longevity of the PRB. Similarly, observations of PRB-2 over several years would be used to assess the accuracy of the model predictions made during its design stage. Once the authors have gathered enough field measurements from the recently constructed PRB extension (PRB-2), its performance will be presented in detail in a future publication.

6. Conclusions

This paper has described the field monitoring of a pilot-scale permeable reactive barrier (PRB) installed in an acid sulfate soil terrain. The overall efficiency and life span of a PRB are governed by its internal (i.e. within the granular mass) and external (upgradient) groundwater characteristics. Rigorous monitoring of the influent and effluent water chemistry, including the time-dependent variation of concentrations of Al and Fe ions, and an evaluation of relevant geo-hydraulic parameters (e.g. reduction in permeability due to clogging) is imperative to ensure the sound performance of a PRB designed to treat acidic groundwater that is attributed to pyrite oxidation. The following specific conclusions can be drawn based on the results of this study.

1. The processes of acid neutralisation and metal removal by limestone aggregates (98% $CaCO_3$) are more consistent and reliable than the previous usage of recycled concrete particles. Based on the results of column experiments, limestone proved to be more effective at neutralising the acidic influent by maintaining a near-neutral pH (6.5 < pH < 7) for 95 days from the beginning of the test. In contrast, recycled concrete aggregates could only sustain a neutral pH range for 63 days.
2. Acid neutralisation and the removal of toxic metals (Al and Fe) by a PRB filled with recycled concrete aggregates were not uniform along the flow path, thus indicating more intensified armouring and clogging at the inlet zone than at the outlet zone. During the past 14 years of monitoring, at least a 31% reduction in acid neutralisation and 48% reduction in hydraulic conductivity could be attributed to significant biogeochemical

clogging at the entrance of the PRB. This implies that the aggregates at the entrance should be replenished every few years to maintain a continual efficiency of the PRB treatment along the influent flow path.

3. Although the PRB produced an effluent that could meet the environmental regulatory standards to date, the noticeable decrease in pH and permeability of the PRB, as well as an increase in the concentration of dissolved metals after mid-2017, could be the tell-tale signs of the PRB's end of life span. Based on the current measurements, an alkaline PRB of such dimensions (18 m x 1.2 m x 3m) that treats acidic groundwater in pyritic floodplains would probably offer effective longevity of at least 10-12 years.
4. It was noteworthy that the upgradient water quality changed significantly because of the fluctuations in the water level, leading to inconsistent acid neutralisation by the alkaline PRB medium. Therefore, an enhanced design of full-scale PRBs will need to capture the rainfall conditions predicted over its life span (say 10 years) in order to sustain an optimum groundwater treatment process.

Acknowledgement

The authors are grateful for funding received from the Australian Research Council (ARC) to support the research in this area. The guidance and support from Dr Ana Heitor throughout the study is also appreciated. The authors also appreciate the assistance received from industry partners, Manildra Shoalhaven Starches Pty Ltd, Paul Amidy from Glencore Assets Pty Ltd., and Geoff McIntosh from Douglas Partners. The support received from the technical officers of UOW during the construction of PRBs is highly appreciated. The efforts of the staff of UTS-TRC and past research work in the field of acid sulfate soils are gratefully acknowledged.

References

ANZECC (Australian and New Zealand Environment Conservation Council) 2000. Australian and New Zealand guidelines for fresh and marine water quality. Australian and New Zealand Environment and Conservation Council and Agriculture and Resource Management Council of Australia and New Zealand, Canberra, 1-103.

Bain J, Blowes D, Smyth D, Ptacek C, Wilkens J & Ludwig R 2006. Permeable reactive barriers for in-situ treatment of arsenic-contaminated groundwater. *Proceedings of the 5th International Conference on Remediation of Chlorinated and Recalcitrant Compounds*. Battelle Press, Columbus, OH, 2006.

Baston G, Clacher A, Heath T, Hunter F, Smith V & Swanton S. 2012. Calcium silicate hydrate (CSH) gel dissolution and pH buffering in a cementitious near field. *Mineralogical Magazine*, 76(8), 3045-3053. https://doi.org/10.1180/minmag.2012.076.8.20

Banasiak L, Indraratna B, Regmi G, Golab A & Lugg G. 2013. Characterisation and assessment of recycled concrete aggregates used in a permeable reactive barrier for the treatment of acidic groundwater. *Geomechanics and Geoengineering,* 8(3)**,** 155-166. https://doi.org/10.1080/17486025.2012.727035

Balintova M. & Petrilakova A. 2011. Study of pH influence on selective precipitation of heavy metals from acid mine drainage. *Chemical Engineering Transactions,* 25**,** 345-350. https://doi.org/10.3303/CET1125058

Bellmann F, Möser B & Stark J. 2006. Influence of sulfate solution concentration on the formation of gypsum in sulfate resistance test specimen. *Cement and Concrete Research,* 36(2)**,** 358-363. https://doi.org/10.1016/j.cemconres.2005.04.006

Berner UR. 1988. Modelling the incongruent dissolution of hydrated cement minerals. *Radiochimica Acta,* 44-45(2)**,** 387-394. https://doi.org/10.1524/ract.1988.4445.2.387

Blowes DW, Ptacek CJ, Benner SG, Mcrae CW, Bennett TA.& Puls RW. 2000. Treatment of inorganic contaminants using permeable reactive barriers. *Journal of Contaminant Hydrology,* 45(2)**,** 123-137. https://doi.org/10.1016/S0169-7722(00)00122-4

Blunden B & Indraratna B. 2000. Evaluation of surface and groundwater management strategies for drained sulfidic soil using numerical simulation models. *Australian Journal of Soil Research,* 38(3)**,** 569-590. https://doi.org/10.1071/SR99018

Cardiano P, Cigala RM, Crea F, Giacobello F, Giuffrè O, Irto A, Lando G & Sammartano S. 2017. Sequestration of Aluminium (III) by different natural and synthetic organic and inorganic ligands in aqueous solution. Chemosphere, 186, 535-545. https://doi.org/10.1016/j.chemosphere.2017.08.013

Cravotta CA & Trahan MK. 1999. Limestone drains to increase pH and remove dissolved metals from acidic mine drainage. *Applied Geochemistry,* 14(5)**,** 581-606. https://doi.org/10.1016/S0883-2927(98)00066-3

Cravotta CA & Watzlaf GR. 2003. Design and performance of limestone drains to increase pH and remove metals from acidic mine drainage. Adapted by DL Naftz, SJ Morrison, JA Davis & CC Fuller (eds), *Handbook of Groundwater Remediation Using Permeable Reactive Barriers***,** 2nd edn, Academic Press, 19-66. https://doi.org/10.1016/B978-012513563-4/50006-2

Ekolu SO & Bitandi LK. 2018. Prediction of longevities of ZVI and pervious concrete reactive barriers using the transport simulation model. *Journal of Environmental Engineering,* 144(9)**,** 04018074. https://doi.org/10.1061/(ASCE)EE.1943-7870.0001402

Fitzpatrick R, Shand P & Hicks W. 2011. Technical guidelines for assessment and management of inland freshwater areas impacted by acid sulfate soils. *CSIRO Land and Water Science Report,* 5**,** 160. https://doi.org/10.5072/83/5849a13e94e13

Gibert O, Assal A, Devlin H, Elliot, T. & Kalin, R. M. 2019. Performance of a field-scale biological permeable reactive barrier for in-situ remediation of nitrate-contaminated groundwater. *Science of the total environment,* 659**,** 211-220. https://doi.org/10.1016/j.scitotenv.2018.12.340

Gillham RW, Vogan J, Gui L, Duchene M.& Son J. 2010. Iron barrier walls for chlorinated solvent remediation. Adapted by H Stroo & Ward C. (eds), *In situ remediation of chlorinated solvent plumes.* Springer. https://doi.org/10.1007/978-1-4419-1401-9_16

Golab AN, Indraratna B, Peterson MA. & Hay S. 2006a. Design of a Permeable Reactive Barrier to Remediate Acidic Groundwater. *ASEG Extended Abstracts,* 2006**,** 1-3. https://doi.org/10.1071/ASEG2006ab051

Golab AN, Peterson M. & Indraratna,B. 2006b. Selection of potential reactive materials for a permeable reactive barrier for remediating acidic groundwater in acid sulphate soil terrains. *Quarterly Journal of Engineering Geology and Hydrogeology,* 39**,** 209-223. https://doi.org/10.1144/1470-9236/05-037

Goyal S. & Sharma D. 2020. CO2 sequestration on cement. Adapted by F Pacheco-Torgal, E Rasmussen, C Granqvist, V Ivanov, A Kaklauskas & S Makonin, (eds), *In situ remediation of chlorinated solvent plume, Start-Up Creation.* Elsevier. https://doi.org/10.1016/B978-0-12-819946-6.00006-0

Groeger J, Hamer K & Schulz HD 2008. The potential for chemical attack by acid sulfate soils in Northern Germany-Combined acid and sulfate attack on concrete, trans. *Beton-und Stahlbetonbau,* 103**,** 563-569. https://doi.org/10.1002/best.200800628

Harris A, Manning M, Tearle W & Tweed C. 2002. Testing of models of the dissolution of cements—leaching of synthetic CSH gels. *Cement and Concrete Research,* 32(5)**,** 731-746. https://doi.org/10.1016/S0008-8846(01)00748-7

Högfors-Rönnholm E, Christel S, Dalhem K, lillhonga ., Engblom S, Österholm P & Dopson M. 2018. Chemical and microbiological evaluation of novel chemical treatment methods for acid sulfate soils. *Science of The Total Environment,* 625**,** 39-49. https://doi.org/10.1016/j.scitotenv.2017.12.287

Hoppe, J, Bain J, Lee D, Hartwig D, Jeen S & Blowes D. 2011. Modeling the Groundwater Flow of a 90 Sr Plume Through a Permeable Reactive Barrier Installed at the Chalk River Laboratories, Chalk River, Ontario, Canada. *The New Uranium Mining Boom.* Springer Geology. https://doi.org/10.1007/978-3-642-22122-4_82

Indraratna B, Regmi G, Nghiem l & A., G. 2010. Performance of a prb for the remediation of acidic groundwater in acid sulfate soil terrain. *Journal Of Geotechnical And Geoenvironmental Engineering, ASCE,* 136(7)**,** 897-906. https://doi.org/10.1061/(ASCE)GT.1943-5606.0000305

Indraratna B, Pathirage PU & Banasiak LJ. 2014a. Remediation of acidic groundwater by way of permeable reactive barrier. *Environmental Geotechnics* 4(4 , 284-298. https://doi.org/10.1680/envgeo.14.00014

Indraratna B, Pathirage PU, Rowe RK & Banasiak L. 2014b. Coupled hydro-geochemical modelling of a permeable reactive barrier for treating acidic groundwater. *Computers and Geotechnics,* 55**,** 429-439. https://doi.org/10.1016/j.compgeo.2013.09.025

Indraratna B, Medawela S, Athuraliya S, Heitor A & Baral P. 2019. Chemical clogging of granular media under acidic groundwater. *Environmental Geotechnics, Special Issue: Testing and Modelling of Complex Rockfill Material.* https://doi.org/10.1680/jenge.18.00143

Indraratna, B, Medawela S, Rowe RK, Thamwattana N & Heitor A. 2020. Biogeochemical Clogging of Permeable Reactive Barriers in Acid Sulfate Soil Floodplain. *Journal of Geotechnical and Geoenvironmental Engineering,* 146(5)**,** 04020015. https://doi.org/10.1061/(ASCE)GT.1943-5606.0002231

Jeen SW, Gillham RW & Przepiora A. 2011. Predictions of long-term performance of granular iron permeable reactive barriers: Field-scale evaluation. *Journal of Contaminant Hydrology,* 123(1-2)**,** 50-64. https://doi.org/10.1016/j.jconhyd.2010.12.006

Li L, Benson CH. & Lawson EM. 2006. Modeling porosity reductions caused by mineral fouling in continuous-wall permeable reactive barriers. *Journal of Contaminant Hydrology,* 83(1-2)**,** 89-121. https://doi.org/10.1016/j.jconhyd.2005.11.004

Maamoun I, Eljamal O, Falyouna O, Eljamal R & Sugihara Y. 2020. Multi-objective optimisation of permeable reactive barrier design for Cr (VI) removal from groundwater. *Ecotoxicology and Environmental Safety,* 200**,** 110773. https://doi.org/10.1016/j.ecoenv.2020.110773

Medawela S, Indraratna B, Pathirage U & Heitor A. 2019. Controlling Soil and Water Acidity in Acid Sulfate Soil Terrains Using Permeable Reactive Barriers. Adapted by Sundaram R, Shahu J, Havanagi V. (eds), *Geotechnics for Transportation Infrastructure.* Springer. https://doi.org/10.1007/978-981-13-6701-4_27

Medawela S & Indraratna B 2020. Computational modelling to predict the longevity of a permeable reactive barrier in an acidic floodplain. *Computers and Geotechnics,* 124**,** 103605. https://doi.org/10.1016/j.compgeo.2020.103605

Nordstrom DK. 1982. Aqueous pyrite oxidation and the consequent formation of secondary iron minerals .Adapted by JA Kittrick, DS Fanning, LR Hossner (eds), *Acid Sulfate Weathering***,** 10, 37-56. https://doi.org/10.2136/sssaspecpub10.c3

NRMMC (National Resource Management Ministerial Council) 2011. Australian Drinking Water Guidelines, National Water Quality Management Strategy, Paper 6. National Health and Medical Research Council, , Commonwealth of Australia, Canberra.

Parkhurst DL & AppeloC 1999. User's guide to PHREEQC (Version 2): A computer program for speciation, batch-reaction, one-dimensional transport, and inverse geochemical calculations. *Water-resources investigations report,* 99**,** 312.

Pathirage U & Indraratna B. 2014. Assessment of optimum width and longevity of a permeable reactive barrier installed in an acid sulfate soil terrain. *Canadian Geotechnical Journal,* 52**,** 999-1004. https://doi.org/10.1139/cgj-2014-0310

Pronk J, De Bruyn J, Bos P & Kuenen J. 1992. Anaerobic growth of Thiobacillus ferrooxidans. *Applied and Environmental Microbiology,* 58(7)**,** 2227-2230. https://doi.org/10.1128/aem.58.7.2227-2230.1992

Puls RW, Paul CJ & Powell RM. 1999. The application of in situ permeable reactive (zero-valent iron) barrier technology for the remediation of chromate-contaminated groundwater: a field test. *Applied Geochemistry,* 14(8)**,** 989-1000. https://doi.org/10.1016/S0883-2927(99)00010-4

Rawlings DE. 2002. Heavy metal mining using microbes 1. *Annual Reviews in Microbiology,* 56**,** 65-91. https://doi.org/10.1146/annurev.micro.56.012302.161052

Rayment G & Higginson FR. 1992. *Australian laboratory handbook of soil and water chemical methods*, Inkata Press Pty Ltd.

Regmi G, Indraratna B & Nghiem LD. 2009. Long-term performance of a permeable reactive barrier in acid sulphate soil terrain. *Water, Air, & Soil Pollution: Focus,* 9**,** 409-419. https://doi.org/10.1007/s11267-009-9230-1

Regmi G, Indraratna B, Nghiem LD & Banasiak, L. 2011. Evaluating waste concrete for the treatment of acid sulphate soil groundwater from coastal floodplains. *Desalination and water treatment,* 32**,** 126-132. https://doi.org/10.5004/dwt.2011.2687

Rimstidt JD & Vaughan DJ. 2003. Pyrite oxidation: a state-of-the-art assessment of the reaction mechanism. *Geochimica et Cosmochimica acta,* 67(5) 873-880. https://doi.org/10.1016/S0016-7037(02)01165-1

Robbins E, Cravotta CA, Savela C & Nord Jr G. 1999. Hydrobiogeochemical interactions inanoxic limestone drains for neutralisation of acidic mine drainage. *Fuel,* 78(2)**,** 259-270. https://doi.org/10.1016/S0016-2361(98)00147-1

Sephton MG. & Webb JA. 2019. The role of secondary minerals in remediation of acid mine drainage by Portland cement. *Journal of hazardous materials,* 367**,** 267-276. https://doi.org/10.1016/j.jhazmat.2018.12.035

Shand P, Appleyard S, Simpson SL, Degens B & Mosley, L. 2018. National Acid Sulfate Soils Guidance: Guidance for the dewatering of acid sulfate soils in shallow groundwater environments. Department of Agriculture and Water Resources, Canberra, ACT. CC BY 4.0.

Singer PC & Stumm W. 1970. Acidic mine drainage: The rate-determining step. *Science,* 167**,** 1121-1123. https://doi.org/10.1126/science.167.3921.1121

List of Figures

Figure 10: Variations in pH along the groundwater flow path of PRB-1 [Data sources: 2006 – 2010 from Indraratna et al. (2010); 2011 – 2013 from Indraratna et al. (2014a)]

Figure 11: Variations of ion concentrations along the groundwater flow path of PRB-1 (a) Ca (c) Al (d) Fe
[Data sources: 2006 – 2010 from Indraratna et al. (2010); 2011 – 2013 from Indraratna et al. (2014a)]

Figure 12: SEM-EDS analysis of recycled concrete aggregates (a) EDS spectra of recycled concrete aggregates (RCA) before used in PRB-1 (b) SEM image of fresh RCA surface before used in PRB-1 (c) Photo of RCA before used in PRB-1 (d) EDS spectra of armoured RCA (e) SEM image of armoured RCA surface (f) Photo of armoured RCA extracted from the inlet of PRB-1 in December 2019

Figure 13: Variation of hydraulic conductivity at the inlet and outlet of PRB-1

Figure 14: Effluent pH of PRB-2 constructed in November 2019

Table 1. Chemistry of groundwater in the Shoalhaven acidic floodplain (Indraratna et al. 2010)

Parameter	Values
pH	3.8
ORP	610 mV
Na^{+}	504.2 mg/L
K^{+}	50.1 mg/L
Ca^{2+}	152.2 mg/L
Mg^{2+}	118 mg/L
Al^{3+}	54 mg/L
Fe^{3+}	9 mg/L
Cl^{-}	849 mg/L
SO_4^{2-}	1350 mg/L

Table 2: Details of instrumentation framework installed for PRB-1 (filled with recycled concrete aggregates) and PRB-2 (filled with limestone)

Instrumentation	No. of instruments		Parameters*	Installation Depth	Other Comments
	PRB-1 (2006)	PRB-2 (2019)			
Observation wells (OWs): (External diameter 50mm; screen length 1.5 m from base)	32	28	pH ORP EC DO	2.5 m	• A portable multi-parameter electrode probe (Hanna Instruments - HI9828) is used to record water quality parameters monthly. • Groundwater samples were collected monthly from the OWs. Following the standard method outlined by Rayment and Higginson (1992), samples were filtered (45 µm) and acid preserved for analysing the concentrations of dissolved cations by inductively coupled plasma optical emission spectroscopy (Agilent 700 series ICP-OES).
Multi-parameter sensor and data logger: (Halytech HydroSpider-2)	2	2	pH ORP EC DO	2.5 m	• Each data logger has been set to record hourly changes of the parameters. The pH/ORP sensor is calibrated every two months and the remaining sensors are calibrated every six months or when required.
Standpipe piezometers: (Filter tip screen length 345 mm)	14	15	Pressure head	2.5 m	• Measured monthly
Vibrating wire piezometers (VWPs) (Roctest PWL low-pressure piezometer)	0	4	Pressure head	2.5 m	• Automated logging (hourly)

*ORP: Oxidation reduction potential, EC: Electrical conductivity DO: Dissolved Oxygen

Table 3: Results of quantitative x-ray diffraction of recycled concrete aggregates (Regmi et al . 2011)

Mineral Phase	Formula	%
Quartz	SiO_2	65.3
Anorthite	$CaAl_2Si_2O_8$	16.8
Albite	$NaAlSi_3O_8$	8.4
Ettringite	$(CaO)_6(Al_2O_3)(SO_3)_3.32H_2O$	4.8
Calcite	$CaCO_3$	4.4
Portlandite	$Ca(OH)_2$	0.3
Goethite	FeOOH	ND*
Gibbsite	$Al(OH)_3$	ND
Boehmite	Al(OOH)	ND

*ND - Not detected

Table 4: Results of quantitative x-ray diffraction of limestone aggregates

Mineral Phase	Formula	%
Calcite	$CaCO_3$	98.2
Dolomite	$CaMg(CO_3)_2$	0.7
Alumina	Al_2O_3	0.2
Boehmite	AlOOH	0.3
Quartz	SiO_2	0.6
Hematite	Fe_2O_3	ND*
Goethite	FeOOH	ND

*ND - Not detected